

THE PHYSICAL NATURE OF $\text{Ly}\alpha$ -EMITTING GALAXIES AT $z = 3.1$ ¹

ERIC GAWISER,^{2,3,4,5} PIETER G. VAN DOKKUM,^{2,3} CARYL GRONWALL,⁴ ROBIN CIARDULLO,⁶ GUILLERMO A. BLANC,⁴
FRANCISCO J. CASTANDER,^{4,7} JOHN FELDMEIER,^{5,8} HAROLD FRANCKE,^{2,4} MARIJN FRANX,⁹ LUTZ HABERZETTL,¹⁰
DAVID HERRERA,^{2,3,11} THOMAS HICKEY,⁶ LEOPOLDO INFANTE,¹² PAULINA LIRA,⁴ JOSÉ MAZA,⁴ RYAN QUADRI,²
ALEXANDER RICHARDSON,^{2,3} KEVIN SCHAWINSKI,¹³ MISCHA SCHIRMER,¹⁴ EDWARD N. TAYLOR,⁹
EZEQUIEL TREISTER,^{2,3,4} C. MEGAN URRY,^{3,11} AND SHANIL N. VIRANI^{2,3}

Received 2005 December 14; accepted 2006 March 23; published 2006 April 12

ABSTRACT

We selected 40 candidate $\text{Ly}\alpha$ -emitting galaxies (LAEs) at $z \approx 3.1$ with observed-frame equivalent widths greater than 150 \AA and inferred emission-line fluxes above $2.5 \times 10^{-17} \text{ ergs cm}^{-2} \text{ s}^{-1}$ from deep narrowband and broadband MUSYC images of the Extended Chandra Deep Field South. Covering 992 arcmin^2 , this is the largest “blank field” surveyed for LAEs at $z \sim 3$, allowing an improved estimate of the space density of this population of $(3 \pm 1) \times 10^{-4} h_{70}^3 \text{ Mpc}^{-3}$. Spectroscopic follow-up of 23 candidates yielded 18 redshifts, all at $z \approx 3.1$. Over 80% of the LAEs are dimmer in continuum magnitude than the typical Lyman break galaxy (LBG) spectroscopic limit of $R = 25.5$ (AB), with a median continuum magnitude $R \approx 27$ and very blue continuum colors, $V-z \approx 0$. Over 80% of the LAEs have the right UVR colors to be selected as LBGs, but only 10% also have $R \leq 25.5$. Stacking the $UBVRIZJK$ fluxes reveals that LAEs have stellar masses $\approx 5 \times 10^8 h_{70}^2 M_{\odot}$ and minimal dust extinction, $A_V \lesssim 0.1$. Inferred star formation rates are $\approx 6 h_{70}^2 M_{\odot} \text{ yr}^{-1}$, yielding a cosmic star formation rate density of $2 \times 10^{-3} h_{70} M_{\odot} \text{ yr}^{-1} \text{ Mpc}^{-3}$. None of our LAE candidates show evidence for rest-frame emission-line equivalent widths $\text{EW}_{\text{rest}} > 240 \text{ \AA}$ that might imply a nonstandard initial mass function. One candidate is detected by *Chandra*, implying an AGN fraction of $2\% \pm 2\%$ for LAE candidate samples. In summary, LAEs at $z \sim 3$ have rapid star formation, low stellar mass, little dust obscuration, and no evidence for a substantial AGN component.

Subject heading: galaxies: high-redshift

Online material: color figures

1. INTRODUCTION

Because $\text{Ly}\alpha$ emission is easily quenched by dust, the $\text{Ly}\alpha$ -emitting galaxies (LAEs) are often characterized as proto-galaxies experiencing their first burst of star formation (Hu & McMahon 1996). However, the differing behavior of $\text{Ly}\alpha$ and continuum photons encountering dust and neutral gas makes it possible for older galaxies to exhibit $\text{Ly}\alpha$ emission when morphology and kinematics favor the escape of these photons (see, e.g., Haiman & Spaans 1999). Hence, the LAEs could

instead represent an older population with actively star-forming regions.

LAEs offer the chance to probe the bulk of the high-redshift galaxy luminosity function, as the strong emission line allows spectroscopic confirmation of objects dimmer than the continuum limit, $R \leq 25.5$. Previous studies of LAEs at $z \sim 3$ have concentrated on known overdensities (Steidel et al. 2000; Hayashino et al. 2004; Venemans et al. 2005) or searches for $\text{Ly}\alpha$ emission near known damped $\text{Ly}\alpha$ absorption systems (Fynbo et al. 2003; see Wolfe et al. 2005 for a review). Blank fields, that is, those not previously known to contain unusual objects or overdensities, have been studied at $z = 3.1$ and $z = 3.4$, covering 468 arcmin^2 (Ciardullo et al. 2002) and 70 arcmin^2 (Cowie & Hu 1998; Hu et al. 1998), respectively. Significant work has been done in recent years on large blank fields at higher redshifts to study the LAE luminosity function at $z = 3.7$ (Fujita et al. 2003), $z = 4.5$ (Hu et al. 1998), $z = 4.9$ (Ouchi et al. 2003; Shimasaku et al. 2003), $z = 5.7$ (Martin & Sawicki 2004; Malhotra & Rhoads 2004; references therein), and $z = 6.5$ (Malhotra & Rhoads 2004). Spectroscopically confirmed samples are small, including 31 LAEs at $z = 3.1$ (Venemans et al. 2005), 18 at $z = 4.5$ (LALA, Dawson et al. 2004), 27 at $z = 5.7$ (Hu et al. 2004; Ouchi et al. 2005), and nine at $z = 6.6$ (Taniguchi et al. 2005). The current investigation expands upon the blank-field survey of Ciardullo et al. (2002) by covering twice the area to a narrowband detection limit 1 mag deeper.

The study of LAEs at $z \approx 3.1$ is a major goal of the Multi-wavelength Survey by Yale-Chile (MUSYC; Gawiser et al. 2006).¹⁵ The Extended Chandra Deep Field South (ECDF-S) has been targeted with deep narrowband imaging and multi-

¹ Based on observations obtained with the Magellan telescopes at Las Campanas Observatory and at Cerro Tololo Inter-American Observatory, a division of the National Optical Astronomy Observatory, which is operated by the Association of Universities for Research in Astronomy, Inc., under cooperative agreement with the National Science Foundation.

² Department of Astronomy, Yale University, New Haven, CT 06520-8101; gawiser@yale.edu.

³ Yale Center for Astronomy and Astrophysics, Yale University, New Haven, CT 06520-8121.

⁴ Departamento de Astronomía, Universidad de Chile, Casilla 36-D, Santiago, Chile.

⁵ National Science Foundation Astronomy and Astrophysics Postdoctoral Fellow.

⁶ Department of Astronomy and Astrophysics, Pennsylvania State University, University Park, PA 16802-6305.

⁷ Institut d'Estudis Espacials de Catalunya, CSIC, Gran Capità 2–4, E-08034 Barcelona, Spain.

⁸ National Optical Astronomy Observatory, Tucson, AZ 85726-6732.

⁹ Sterrewacht Leiden, Postbus 9513, NL-2300 RA Leiden, Netherlands.

¹⁰ Astronomisches Institut der Ruhr-Universität-Bochum, Universitätsstrasse 150, D-44780 Bochum, Germany.

¹¹ Department of Physics, Yale University, New Haven, CT 06520-8120.

¹² Departamento de Astronomía y Astrofísica, Pontificia Universidad Católica de Chile, Casilla 306, Santiago 22, Chile.

¹³ Astrophysics, University of Oxford, Keble Road, Oxford OX1 3RH, UK.

¹⁴ Institut für Astrophysik und Extraterrestrische Forschung, Universität Bonn, Auf dem Hügel 71, D-53121 Bonn, Germany.

¹⁵ See <http://www.astro.yale.edu/MUSYC>.

TABLE 1

DETECTION LIMITS FOR MUSYC ECDF-S IMAGES	
Band	Limit
NB5000	25.5
<i>U</i>	26.0
<i>B</i>	26.9
<i>V</i>	26.4
<i>R</i>	26.4
<i>I</i>	24.6
<i>z'</i>	23.6
<i>J</i>	22.7
<i>K</i>	22.0

NOTE.—Limits are 5σ for point sources (AB magnitudes).

object spectroscopy, complemented by deep broadband *UBVRIzJK* and public *Chandra* ACIS-I imaging. These multi-wavelength data make it possible to study the physical nature of LAEs and to distinguish star formation from active galactic nuclei (AGNs) as the source of their emission. We assume a Λ CDM cosmology consistent with *WMAP* results (Bennett et al. 2003), with $\Omega_m = 0.3$, $\Omega_\Lambda = 0.7$, and $H_0 = 70 h_{70} \text{ km s}^{-1} \text{ Mpc}^{-1}$. All magnitudes are given in the AB95 system (Fukugita et al. 1996).

2. OBSERVATIONS

Our narrowband imaging of the ECDF-S was obtained using the narrowband 5000 Å filter (NB5000; 50 Å FWHM) with the CTIO 4 m telescope and MOSAIC II on several nights from 2002 to 2004 for a total of 29 hr of exposure time. Our *UBVRI* imaging results from combining public images taken with the ESO 2.2 m and WFI by the ESO Deep Public Survey and COMBO-17 teams (Erben et al. 2005; Hildebrandt et al. 2005; Arnouts et al. 2001; Wolf et al. 2004). Our *z'* imaging was taken with the CTIO 4 m and MOSAIC II on 2005 January 15. Details of our optical images will be presented in E. Gawiser et al. (2006, in preparation). Our *JK* images of the ECDF-S were obtained with the CTIO 4 m and ISPI on several nights during 2003–2004 and will be described in E. N. Taylor et al. (2006, in preparation). The final images cover $31'.5 \times 31'.5 = 992 \text{ arcmin}^2$ centered on the *Chandra* Deep Field South and were processed through the MUSYC photometric pipeline to generate APCORR (corrected aperture) fluxes and uncertainties as described in Gawiser et al. (2006). Table 1 gives our source detection depths.

Multiobject spectroscopy of 23 LAE candidates was performed with the IMACS instrument on the Magellan Baade Telescope on 2003 October 26–27, 2004 October 7–8, and 2005 February 4–7. The 300 line mm^{-1} grism was used with 1".2 slitlets to cover 4000–9000 Å at a resolution of 7.8 Å. Details of our spectroscopy will be given in P. Lira et al. (2006, in preparation).

3. CANDIDATE SELECTION

The greatest challenge in selecting LAEs at $z \approx 3.1$ is to minimize contamination from $z \approx 0.34$ galaxies exhibiting emission lines in [O II] $\lambda 3727$. These interlopers can be avoided by requiring a high equivalent width ($>150 \text{ \AA}$ in the observed frame), which eliminates all but the rarest [O II] emitters (Terlevich et al. 1991; Stern et al. 2000). Contamination from [O III] $\lambda 5007$ is minimal at these wavelengths, as the volume for extragalactic emitters is small, and Galactic planetary nebulae are very rare at such high Galactic latitudes ($b = -54^\circ$).

Selecting LAEs requires an estimate of the continuum at the wavelength of the narrowband filter, so we tested weighted sums

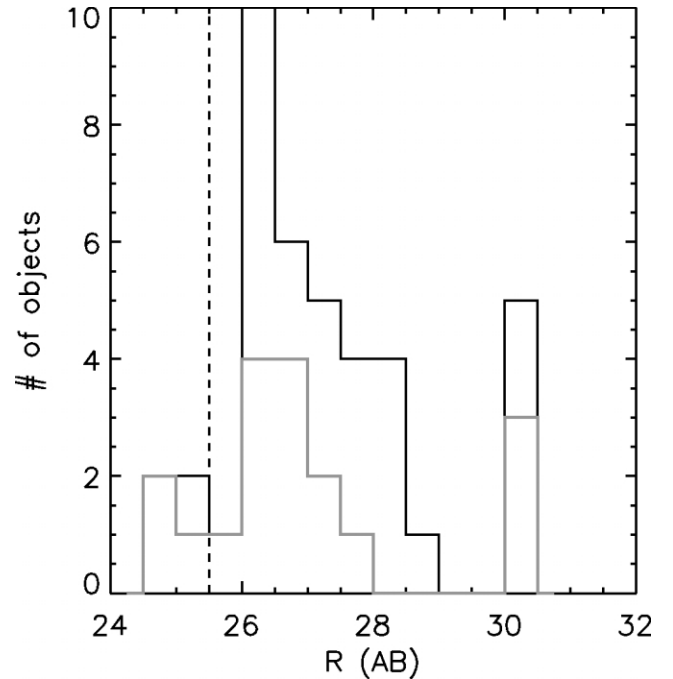


FIG. 1.—Distribution of *R*-band magnitudes for candidate LAEs (black histogram) and the subset of confirmed LAEs (gray histogram), with the typical spectroscopic limit of $R = 25.5$ marked by the dashed vertical line. Objects with negative fluxes in *R* were assigned $R = 30$. [See the electronic edition of the *Journal* for a color version of this figure.]

of the *B* and *V* flux densities and found that $f_v^{BV} = (f_v^B + f_v^V)/2$ minimizes the scatter in predicting the NB5000 flux density of typical objects. The “narrowband excess” in magnitudes, $BV - \text{NB5000}$, was then used to select the candidate LAEs with $BV - \text{NB5000} > 1.5$, corresponding to $\text{EW}_{\text{obs}} > 150 \text{ \AA}$. When the broadband fluxes are small, significant errors in the equivalent width estimate may result, and a small fraction of the numerous objects without emission lines, that is, with $BV - \text{NB5000} \approx 0$, could enter the “narrowband excess” sample. To avoid both types of interlopers, we calculated a formal uncertainty in the $BV - \text{NB5000}$ color in magnitudes, $\sigma_{BV - \text{NB}}$, and required candidate LAEs to have $(BV - \text{NB5000}) - \sigma_{BV - \text{NB}} > 1.5$ and $(BV - \text{NB5000}) - (3\sigma_{BV - \text{NB}}) > 0$. The latter criterion is similar to the color excess requirement of Bunker et al. (1995), but our color uncertainties are object specific and account for variation in image depth across the field (see Gawiser et al. 2006). To make spectroscopic confirmation feasible, we also required $\text{NB5000} < 25.0$, implying an emission-line flux $\geq 2.5 \times 10^{-17} \text{ ergs cm}^{-2} \text{ s}^{-1}$. Visual inspection to eliminate false narrowband detections caused by CCD defects or cosmic-ray residuals resulted in 40 candidate LAEs. Twenty-three of these have been observed spectroscopically, yielding 18 confirmations in which the Ly α emission line was clearly detected in both the two-dimensional and extracted spectra and no other emission lines were visible across the full optical spectrum. We tested the procedure by observing lower equivalent width objects and found several [O II] $\lambda 3727$ emitters; all of these interlopers exhibit clear emission lines in H β , [O III] $\lambda \lambda 4959, 5007$, and H α . Five of the LAE candidate spectra fail to show emission lines.

4. RESULTS

Figure 1 shows the distribution of candidate and confirmed LAE *R*-band continuum magnitudes versus the “spectroscopic” Lyman break galaxy (LBG) limit of $R \leq 25.5$ (Steidel et al. 2003). Our study of LAEs is able to observe objects much

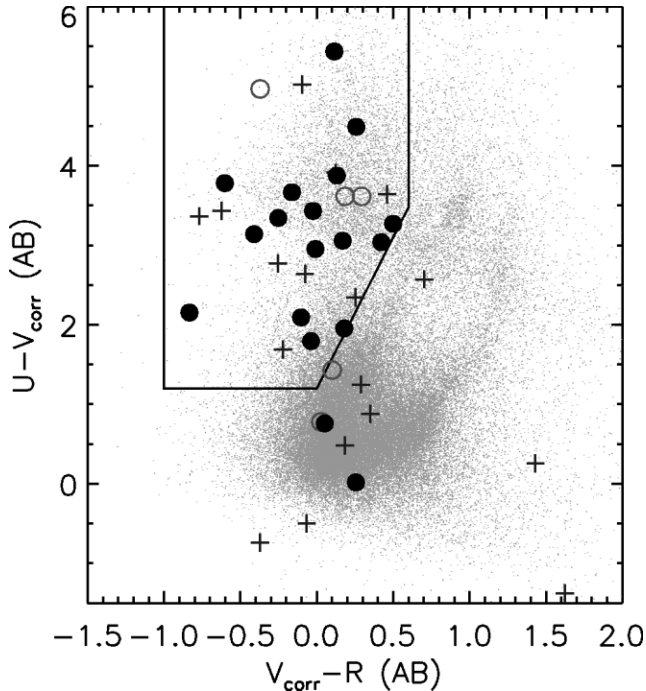


FIG. 2.—*UVR* color-color plot of confirmed LAEs (filled circles), candidate LAEs with spectroscopy but no confirmed redshift (open circles), and candidate LAEs without spectroscopy (plus signs) vs. distribution of the entire 84,410 object optical catalog (dots). The polygonal region at upper left is the Lyman break galaxy selection region. [See the electronic edition of the *Journal* for a color version of this figure.]

dimmer than this, with a median magnitude $R \sim 27$. Thirty-six of 40 candidates and 15 of 18 confirmed LAEs have $R > 25.5$, showing the efficacy of LAE selection in identifying objects from the bulk of the high-redshift galaxy luminosity function. Figure 2 shows $UV_{\text{corr}}R$ colors of our LAE candidates versus the LBG selection region determined by Gawiser et al. (2006), where V_{corr} refers to the V -band magnitude after subtracting the flux contributed by the Ly α emission lines. Only two out of 18 confirmed LAEs fall within the $R \leq 25.5$ “spectroscopic” LBG sample, but 16 out of 18 fall within the color selection region. About half of our candidate LAEs would meet the $R < 27$ magnitude limit of the “photometric” LBG sample explored by Sawicki & Thompson (2005), and these objects should make up 5% of their sample.

In order to investigate the full spectral energy distribution (SED) of the LAEs, which are too dim to obtain individual detections in our near-IR photometry, we measured stacked fluxes for the confirmed sample; the results of SED modeling are shown in Figure 3. Bruzual & Charlot (2003) population synthesis models were used, with constant star formation rate, a Salpeter (1955) initial mass function (IMF) from 0.1 to 100 M_{\odot} , solar metallicity, and Calzetti et al. (1997) dust reddening (see, e.g., Förster Schreiber et al. 2004; van Dokkum et al. 2004). Uncertainties in the stacked photometry were determined using bootstrap resampling and are close to the formal errors calculated from the reported APCORR flux uncertainties. Parameter uncertainties were computed by means of a Monte Carlo analysis in which the stacked fluxes were varied within their uncertainties to yield a probability distribution of best-fit parameters. The age of the stellar population is weakly constrained and has been restricted to the physically reasonable range $10 \text{ Myr} \leq t_* \leq 2 \text{ Gyr}$. The best-fit parameters shown in Figure 3 correspond to minimal dust extinction, significant star formation rates ($5 h_{70}^{-2} M_{\odot} \text{ yr}^{-1} \leq \text{SFR} \leq 23 h_{70}^{-2} M_{\odot} \text{ yr}^{-1}$ at

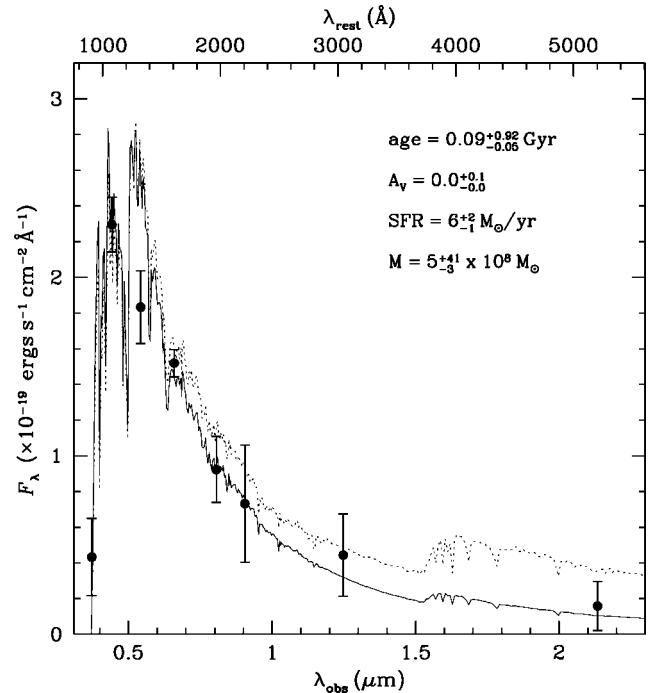


FIG. 3.—*UBVRIzJK* broadband photometry (average flux density of stacked sample) of confirmed LAEs along with the best-fit model from SED fitting (solid curve), with model parameters listed. The dotted curve shows a maximally old model with stellar population age fixed to 2 Gyr (the age of the universe at $z = 3.1$), $A_v = 0.1$, $\text{SFR} = 7 h_{70}^{-2} M_{\odot} \text{ yr}^{-1}$, and $M_* = 1.1 \times 10^{10} h_{70}^{-2} M_{\odot}$.

95% confidence), and low stellar mass (the 95% confidence upper limit is $M_* = 8.5 \times 10^9 h_{70}^{-2} M_{\odot}$). The LAEs appear to have much less dust and stellar mass than the $\sim 500 \text{ Myr}$ old, $A_v \approx 1$, $\sim 2 \times 10^{10} M_{\odot}$ LBG population (Shapley et al. 2001) or the $\sim 2 \text{ Gyr}$ old, $A_v \approx 2.5$, $\sim 10^{11} M_{\odot}$ distant red galaxy population (Förster Schreiber et al. 2004). The SFRs of the confirmed LAEs inferred from their Ly α luminosities average $5 h_{70}^{-2} M_{\odot} \text{ yr}^{-1}$ and from their rest-frame UV continuum luminosities average $9 h_{70}^{-2} M_{\odot} \text{ yr}^{-1}$. The consistency of these values with the best-fit SFR from SED modeling implies minimal dust extinction.

To check for AGN contamination of our LAE candidate sample, we have looked for *Chandra* detections of these objects. One LAE candidate has an X-ray detection in the catalogs of Virani et al. (2006) and Lehmer et al. (2005a), with a 0.5–8 keV luminosity of $10^{44} \text{ ergs s}^{-1}$. No other candidates showed individual detections, so we removed this object and performed a stacking analysis (e.g., Rubin et al. 2004; Lehmer et al. 2005b), which resulted in a nondetection of the entire population. Using the conversion between SFR and X-ray flux given by Ranalli et al. (2003), the upper limit on the average star formation rate per object is $200 h_{70}^{-2} M_{\odot} \text{ yr}^{-1}$, which is clearly consistent with the observed SFR. None of our LAE spectra show broad emission-line widths ($>1000 \text{ km s}^{-1}$) that would be inconsistent with the energetics of star formation. We therefore expect that very few LAE candidates contain luminous AGNs that dominate their Ly α or continuum emission.

5. DISCUSSION

Our survey covers $31.5 \times 31.5 \times (\Delta z = 0.04)$, or $59 \times 59 \times 38 h_{70}^{-3} \text{ Mpc}^3$, yielding an LAE number density of $(3 \pm 1) \times 10^{-4} h_{70}^3 \text{ Mpc}^{-3}$, equivalent to $4000 \pm 1600 \text{ deg}^{-2}$ per unit redshift. The survey volume was computed using a filter bandpass FWHM = 50 Å, and the five candidates without confirmed red-

shifts were assumed to be LAEs. The error bars account for variations in the LAE abundance within our survey volume caused by large-scale structure, assuming a bias of 2. The true uncertainties could be bigger given the large fluctuations in density observed for LAEs at $z = 4.9$ by Shimasaku et al. (2004). Combining the measured number density and using the best-fit star formation rate per object of $6 h_{70}^2 M_{\odot} \text{ yr}^{-1}$, we find a cosmic SFR density of $2 \times 10^{-3} h_{70} M_{\odot} \text{ yr}^{-1} \text{ Mpc}^{-3}$. This is significantly less than the LBG SFR density (Steidel et al. 1999), but it underestimates the total LAE contribution because of our requirements of high equivalent width and relatively bright NB5000 flux, designed to select a pure sample amenable to spectroscopic confirmation. A detailed calculation of the LAE luminosity function at $z \approx 3.1$, which can be integrated to give a fuller estimate of the SFR density, will be given in C. Gronwall et al. (2006, in preparation).

The number density, stellar masses, SFRs, and median UV continuum fluxes found for LAEs are within a factor of 3 of those predicted by Le Delliou et al. (2005, 2006); the agreement is even better when our equivalent width threshold is accounted for. The only strong disagreement seen versus these models is their claimed escape fraction of 0.02 for Ly α photons versus our lower limit of 0.2 (and best fit of 0.8) implied by the comparison of SFRs determined from the observed Ly α luminosities and SED modeling. This discrepancy could be resolved by using a larger escape fraction and a standard IMF instead of the top-heavy IMF assumed in the models.

Our determination that $z = 3.1$ LAEs are predominantly blue contrasts with the results of Stiavelli et al. (2001) and Pascarelle et al. (1998) that LAEs in blank fields at $z \approx 2.4$ are typically red, $B-I \approx 1.8$. This differs from the median value of $V_{\text{corr}} - z \approx 0.1$ for our spectroscopically confirmed LAEs and the median color $V-I \approx 0.1$ measured by Venemans et al. (2005). The difference seems unlikely to be caused by

evolution in the LAE population from $z = 3.1$ to $z = 2.4$ given the small increase in the age of the universe.

At $z = 4.5$, LALA (Malhotra & Rhoads 2002) reported that a majority of LAE candidates had $EW_{\text{rest}} > 240 \text{ \AA}$, providing evidence of a top-heavy IMF possibly caused by Population III stars, although equivalent widths this high could also result from highly anisotropic radiative transfer due to the differing effects of dust and gas on Ly α and UV continuum photons. This photometric measurement is sensitive to considerable scatter when the sample is selected in the narrowband and the broadband imaging is shallow, as broadband nondetections can receive extremely large implied equivalent widths, and this is guaranteed to occur for any spurious narrowband detections. Indeed, when 2σ upper limits on the continuum flux were used, only 10% of their $z = 4.5$ sample had such high EWs, and $\sim 20\%$ of the confirmed objects have $EW_{\text{rest}} > 240 \text{ \AA}$ (Dawson et al. 2004). We do not find equivalent widths this high for any of our LAE candidates at $z = 3.1$. The difference might reveal evolution in the LAE population, or it could be the result of small number statistics.

We acknowledge the referee, Andrew Bunker, for helpful comments that improved this Letter. We thank James Rhoads and Masami Ouchi for valuable conversations. We are grateful for support from Fundación Andes, the FONDAP Centro de Astrofísica, and the Yale astronomy department. This material is based upon work supported by the National Science Foundation under grants AST 02-01667, 01-37927, 00-71238, and 03-02030 awarded to E. G., C. G., R. C., and J. F., respectively. This work was supported in part by NASA grant HST-GO-09525.13-A.

Facilities: Blanco(MOSAIC II), Magellan:Baade(IMACS)

REFERENCES

- Arnouts, S., et al. 2001, *A&A*, 379, 740
 Bennett, C. L., et al. 2003, *ApJS*, 148, 1
 Bruzual, G., & Charlot, S. 2003, *MNRAS*, 344, 1000
 Bunker, A. J., Warren, S. J., Hewett, P. C., & Clements, D. L. 1995, *MNRAS*, 273, 513
 Calzetti, D., Meurer, G. R., Bohlin, R. C., Garnett, D. R., Kinney, A. L., Leitherer, C., & Storchi-Bergmann, T. 1997, *AJ*, 114, 1834
 Ciardullo, R., Feldmeier, J. J., Krellove, K., Jacoby, G. H., & Gronwall, C. 2002, *ApJ*, 566, 784
 Cowie, L. L., & Hu, E. M. 1998, *AJ*, 115, 1319
 Dawson, S., et al. 2004, *ApJ*, 617, 707
 Erben, T., et al. 2005, *Astron. Nachr.*, 326, 432
 Förster Schreiber, N. M., et al. 2004, *ApJ*, 616, 40
 Fujita, S. S., et al. 2003, *AJ*, 125, 13
 Fukugita, M., Ichikawa, T., Gunn, J. E., Doi, M., Shimasaku, K., & Schneider, D. P. 1996, *AJ*, 111, 1748
 Fynbo, J. P. U., Ledoux, C., Möller, P., Thomsen, B., & Burud, I. 2003, *A&A*, 407, 147
 Gawiser, E., et al. 2006, *ApJS*, 162, 1
 Haiman, Z., & Spaans, M. 1999, *ApJ*, 518, 138
 Hayashino, T., et al. 2004, *AJ*, 128, 2073
 Hildebrandt, H., et al. 2005, *A&A*, 441, 905
 Hu, E. M., Cowie, L. L., Capak, P., McMahon, R. G., Hayashino, T., & Komiyama, Y. 2004, *AJ*, 127, 563
 Hu, E. M., Cowie, L. L., & McMahon, R. G. 1998, *ApJ*, 502, L99
 Hu, E. M., & McMahon, R. G. 1996, *Nature*, 382, 231
 Le Delliou, M., Lacey, C., Baugh, C. M., Guiderdoni, B., Bacon, R., Courtois, H., Sousbie, T., & Morris, S. L. 2005, *MNRAS*, 357, L11
 Le Delliou, M., Lacey, C. G., Baugh, C. M., & Morris, S. L. 2006, *MNRAS*, 365, 712
 Lehmer, B. D., et al. 2005a, *ApJS*, 161, 21
 ———. 2005b, *AJ*, 129, 1
 Malhotra, S., & Rhoads, J. E. 2002, *ApJ*, 565, L71
 ———. 2004, *ApJ*, 617, L5
 Martin, C. L., & Sawicki, M. 2004, *ApJ*, 603, 414
 Ouchi, M., et al. 2003, *ApJ*, 582, 60
 ———. 2005, *ApJ*, 620, L1
 Pascarelle, S. M., Windhorst, R. A., & Keel, W. C. 1998, *AJ*, 116, 2659
 Ranalli, P., Comastri, A., & Setti, G. 2003, *A&A*, 399, 39
 Rubin, K. H. R., van Dokkum, P. G., Coppi, P., Johnson, O., Förster Schreiber, N. M., Franx, M., & van der Werf, P. 2004, *ApJ*, 613, L5
 Salpeter, E. E. 1955, *ApJ*, 121, 161
 Sawicki, M., & Thompson, D. 2005, *ApJ*, 635, 100
 Shapley, A. E., Steidel, C. C., Adelberger, K. L., Dickinson, M., Giavalisco, M., & Pettini, M. 2001, *ApJ*, 562, 95
 Shimasaku, K., et al. 2003, *ApJ*, 586, L111
 ———. 2004, *ApJ*, 605, L93
 Steidel, C. C., Adelberger, K. L., Giavalisco, M., Dickinson, M., & Pettini, M. 1999, *ApJ*, 519, 1
 Steidel, C. C., Adelberger, K. L., Shapley, A. E., Pettini, M., Dickinson, M., & Giavalisco, M. 2000, *ApJ*, 532, 170
 ———. 2003, *ApJ*, 592, 728
 Stern, D., Bunker, A., Spinrad, H., & Dey, A. 2000, *ApJ*, 537, 73
 Stiavelli, M., Scarlata, C., Panagia, N., Treu, T., Bertin, G., & Bertola, F. 2001, *ApJ*, 561, L37
 Taniguchi, Y., et al. 2005, *PASJ*, 57, 165
 Terlevich, R., Melnick, J., Masegosa, J., Moles, M., & Copetti, M. V. F. 1991, *A&AS*, 91, 285
 van Dokkum, P. G., et al. 2004, *ApJ*, 611, 703
 Venemans, B. P., et al. 2005, *A&A*, 431, 793
 Virani, S. N., Treister, E., Urry, C. M., & Gawiser, E. J. 2006, *AJ*, 131, 2373
 Wolf, C., et al. 2004, *A&A*, 421, 913
 Wolfe, A. M., Gawiser, E., & Prochaska, J. X. 2005, *ARA&A*, 43, 861